



Thermal electrocyclization reactions II: benzooctatetraenes and benzodecapentaenes

Dragana Vuk ^a, Željko Marinić ^b, Krešimir Molčanov ^c, Davor Margetić ^{d,*}, Irena Škorić ^{a,*}

^a Department of Organic Chemistry, Faculty of Chemical Engineering and Technology, University of Zagreb, 10000 Zagreb, Croatia

^b NMR Centre, Ruder Bošković Institute, Bijenička cesta 54, 10001 Zagreb, Croatia

^c Division of Physical Chemistry, Ruder Bošković Institute, Bijenička cesta 54, 10001 Zagreb, Croatia

^d Laboratory for Physical-Organic Chemistry, Division of Organic Chemistry and Biochemistry, Ruder Bošković Institute, Bijenička cesta 54, 10001 Zagreb, Croatia

ARTICLE INFO

Article history:

Received 4 October 2013

Received in revised form 29 November 2013

Accepted 10 December 2013

Available online 18 December 2013

Keywords:

Polyenes

Electrocyclizations

Reaction mechanism

Rearrangements

DFT calculations

ABSTRACT

Thermal electrocyclization reactions of benzoctatetraenes and benzodecapentaenes substituted with R=H, Cl, and methyl were studied experimentally and computationally. Methyl and unsubstituted benzoctatetraenes and benzodecapentaenes give the [4.2.0]bicyclooctadiene products by $8\pi,6\pi$ -electrocyclization. Chlorine substitution led to thermal rearrangement of the initially formed $8\pi,6\pi$ -electrocyclization intermediates to give unprecedented products.

© 2013 Elsevier Ltd. All rights reserved.

1. Introduction

Dienes and polyenes are compounds, which intervene in a large number of organic reactions, and are constituents of a large number of natural and human-made compounds, including terpenes, cholesterol, and vitamin A.¹ Characteristic type of reactions for conjugated dienes and polyenes are electrocyclizations, which are synthetically important and believed to be involved in biosynthesis of many natural compounds.² Among them, thermal 6π electrocyclizations of conjugated trienes are the most common of all electrocyclizations employed in the synthesis. In such process, all-carbon, as well as heterocyclic products could be formed.^{3,4} Such reactions lead to conjugated cyclohexadiene units and, although thermodynamically favorable, usually require activation by relatively high temperatures. The cyclohexadiene products can participate in further reactions, such as Diels–Alder cycloadditions, and such reaction cascades form extremely complex molecular architectures.

The $8\pi,6\pi$ electrocyclic cascade (sometimes referred to as Black's cascade) is arguably the most elegant display of the power

of electrocyclization reactions in nature. This tandem reaction sequence involves a cascade of thermally induced 8π , followed by 6π electrocyclizations leading directly to compounds that contain the bicyclo[4.2.0]octa-2,4-diene ring system.⁵ 1,3,5,7-Octatetraenes in which the two internal olefins have the Z-configuration are thermally unstable with respect to the $8\pi,6\pi$ electrocyclization cascade, which explains their tendency to undergo further pericyclic reactions and scarce occurrence of this motif in natural products.

Natural products that arise from $8\pi,6\pi$ electrocyclizations represented by SNF4435 C, ocellapyrone A, and elysiapyrone A, have sparked significant synthetic activity, which has led to a better understanding of electrocyclization cascades and polyene chemistry in general and preparation of natural products, such as shimalactones,⁶ and pre-kingianin A.⁷

As a part of our ongoing interest in reaction mechanisms⁸ and intramolecular photocycloaddition reactions of substituted hexatrienes with one double bond incorporated into the benzene ring⁹ we recently reported synthesis and photocycloadditions of novel o-butadienylstyrenes.¹⁰ In continuation of this work we here present results of thermal rearrangements of benzoctatetraenes (**1–2**) and benzodecapentaenes (**6–8**) possessing substituents at 2-position(s) of polyene moiety.

The aim of this account is to study the influence of substitution patterns on the electrocyclization processes of conjugated

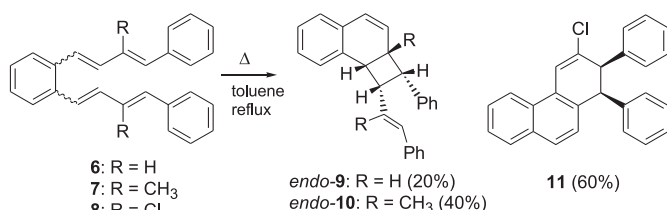
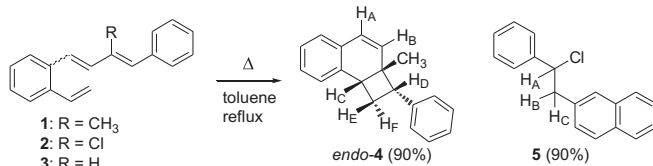
* Corresponding authors. Tel.: +385 1 456 1008; fax: +385 1 468 0195; e-mail addresses: margedit@irb.hr (D. Margetić), iskoric@fkit.hr (I. Škorić).

tetraenes, in which substituents are positioned at the 2-position(s) of conjugated polyenes. In our previous paper, influence of terminal substituents on the product *endo/exo* selectivity was investigated.¹¹

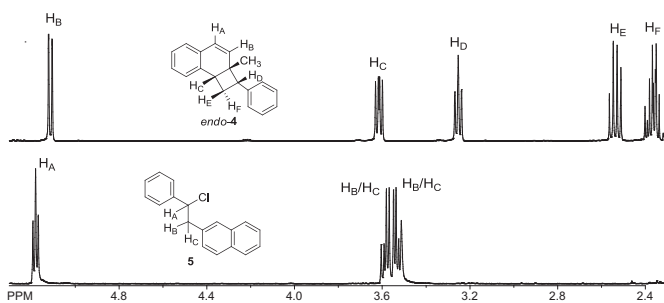
2. Results and discussion

2.1. Experimental study

The starting compounds **1**, **2**, and **6–8** (Schemes 1 and 2) were prepared employing one-pot synthetic approach based on double Wittig reaction, starting from an aromatic diphosphonium salt and two different aldehydes as mixtures of two (compounds **1** and **2**) or three geometric isomers (compounds **6–8**) according to the procedures described in previous papers for heteroarylstilbene derivatives.¹² Using commercially available (*E*) isomers of the α -chloro-cinnamaldehyde and α -methyl-cinnamaldehyde, the second double bond (looking from the *ortho* substituted central benzene ring) was introduced in the starting compounds **1**, **2**, and **6–8** retaining the (*E*) configuration. Hence, the number of the geometric isomers was reduced; the reaction mixtures contain *cis*- and *trans*-isomers of **1** and **2**, and *cis,cis*-, *cis,trans*-, and *trans,trans*-isomers of **6–8** (only the first double bond connected to the *ortho* substituted central benzene ring is designated). By proper addition strategy of these aldehydes, formaldehyde and base the starting compounds **1**, **2**, and **6–8** were obtained in very good yields (51–91%).¹³



Thermal reactions of benzoctatetraenes **1** and **2** are shown in Scheme 1. Upon refluxing **1** or **2** in toluene (111 °C, 20 h), products *endo*-**4** (90%) and **5** (90%) were obtained. Obtained results for α -methyl substitution at the butadiene unit are expected (product *endo*-**4**), while chloro-derivative **2** differs from those obtained in our previous paper for unsubstituted **3**. The structures of products *endo*-**4** and **5** were elucidated using NMR spectroscopy (Fig. 1) and



additionally confirmed for **5** by X-ray crystallography (Fig. 2). Stereochemistry of the *endo*-**4** isomer was deduced from 2D COSY, NOESY, and HSQC NMR experiments, the most indicative being NOESY correlations (Supplementary data).

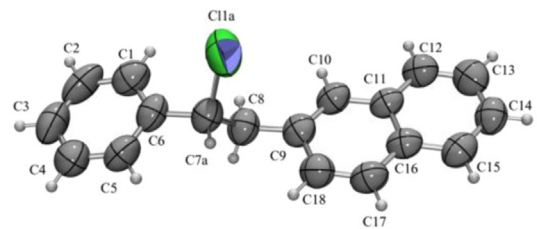


Fig. 2. ORTEP-3¹⁴ drawing of thermal product **5**. Displacement ellipsoids are drawn for the probability of 30% and hydrogen atoms are shown as spheres of arbitrary radii. Only R enantiomer is shown for **5**.

Replacement of the α -methyl group in **1** with chlorine in substrate **2** led to an unusual reaction and only one stereomeric thermal product **5** was obtained (toluene, 16 h, in 90% yield, Scheme 1). On reflux in benzene (80 °C, 16 h) the *cis*-**1** isomer from mixture of isomers was converted also to the *endo*-**4**, but in 65% yield and the *cis*-**2** from mixture of isomers was converted also to **5** but in 80% yield, indicating that a higher temperature is required for the *trans/cis* isomerization of *trans*-**1**. It was found that the *cis*-**1** reacts thermally even in the photochemical reaction¹¹ giving *endo*-**4** as the minor product, aside of major photochemical product. Refluxing of the mixture of isomers of **1** at higher temperature in xylene (144 °C, 16 h) resulted in complete disappearance of the reactant, with only traces of *endo*-**4** present, presumably due to ring cleavage to methyl-naphthalene and styrene. This was corroborated by analysis of ^1H NMR spectra of the thermolysis product of **1** in xylene, which showed only presence of characteristic signals for methyl-naphthalene and styrene and the unreacted *trans*-**1**. Furthermore, GC/MS analysis of a sample after the thermal reaction of mixture of isomers of **1** showed exclusive presence of *trans*-**1** isomer, along with the new signals (M^+ 104 and 142), which are associated to styrene and 2-methyl-naphthalene. GC/MS analysis of a sample obtained after the thermolysis of the chloro-derivative **2** did not show any MS signal, which can be attributed to naphthalene, chloro-naphthalene or styrene (M^+ 128, 162, and 104). This additional information highlights the difference in the thermolysis reaction mechanism of **2** in comparison with the methyl derivative **1**.

The compound **5** possesses one stereogenic center, and crystallizes as a racemate (in the centrosymmetric space group P_{21}/c). However, enantiomeric disorder is present in the crystals, with molecules of both enantiomers occupying the same crystallographic position (with occupancies 0.68 and 0.32, respectively). Since the geometries of both enantiomers are similar, the disorder can be described as two different positions of the stereogenic Cl1–C7–H7 group: the component designated as a (i.e., Cl1a–C7a–H7a) has *R* configuration (Fig. 2), while the component b (i.e., Cl1b–C7b–H7b) has *S* configuration. Crystal packing is achieved only through C–H \cdots π interactions (Table 1).

Further extension of conjugated system to benzodecapentaenes **6–8** shows similar thermal reactivity as observed for **1** and **2** (Scheme 2) in toluene. In the case of thermolysis of mixtures of *cis,cis*-**6–8** and *cis,trans*-**6–8**, unsubstituted and methyl substituted benzodecapentaenes **6** and **7** produced related $8\pi,6\pi$ -electrocyclization products *endo*-**9** and *endo*-**10**. Again, polyene substitution with chlorine affected the reactivity leading to the isolation of an entirely different product **11**, whose structure was

Table 1

Geometric parameters of the C–H···π and interactions in crystal structures of **5** and **11**

	X···Cg /Å	γ /° ^a	C–X···Cg /°	C···Cg /Å	Symm. op. on Cg
<i>Compound 5</i>					
C2–H2···C1 → C6	2.93	10.82	134	3.630(6)	–x, 1/2+y, –1/2-z
C5–H5···C11 → C16	2.97	16.04	129	3.627(5)	x, 1/2-y, –1/2+z
C17–H17···C11 → C1	2.94	15.46	130	3.602(5)	1-x, –1/2+y, 1/2-z
<i>Compound 11</i>					
C3–H3···C7 → C12	2.84	17.17	164	3.788(3)	1-x, –y, –z
C11–H11···C15 → C20	2.87	3.61	154	3.733(4)	–x, 1-y, –z
C25–H25···C4 → C13	2.83	10.56	154	3.684(4)	1-x, 1-y, –z

^a γ =angle defined by a line connecting center of gravity of the aromatic ring with H atom and the normal to the aromatic ring.

determined by NMR spectroscopy (Fig. 3, as well as of products *endo*-**9** and *endo*-**10**) and proven by X-ray crystallography (Fig. 4). Stereochemistry of the *endo*-**8** and *endo*-**10** isomers was deduced from 2D COSY, NOESY, and HSQC NMR experiments, the most indicative being NOESY correlations (see Supplementary data). Furthermore, GC/MS analysis of a sample after the thermal reaction of mixture of isomers of **6** showed presence of only *trans*-**6** isomer, along with the new signals (M^+ 128 and 206), which are associated to naphthalene and 1,4-diphenyl-1,3-butadiene, respectively. Refluxing of the mixture of isomers of **6–8** in benzene did not show any reaction after 8 h, and in xylene (144 °C, 8 h) resulted in cleavage and disappearance of the products *endo*-**9**, *endo*-**10** and **11**, respectively (same as in toluene).

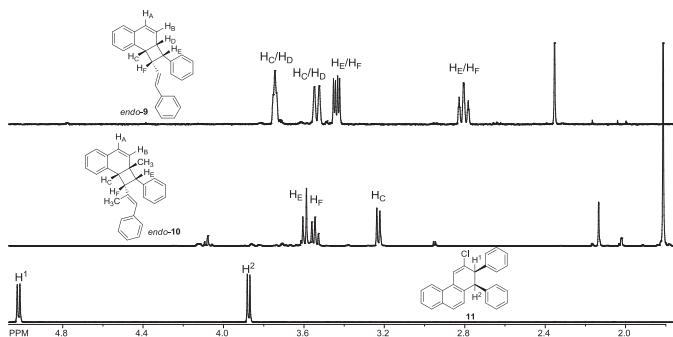


Fig. 3. ^1H NMR spectra of thermal products *endo*-**9**, *endo*-**10**, and **11** (aliphatic region).

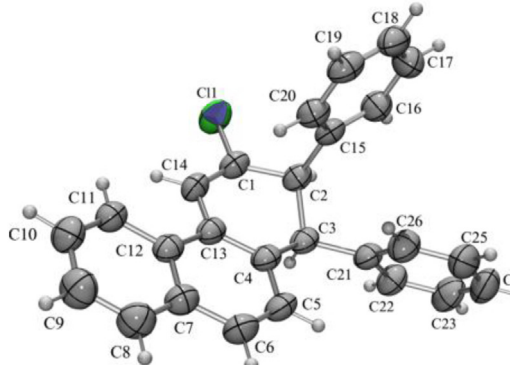
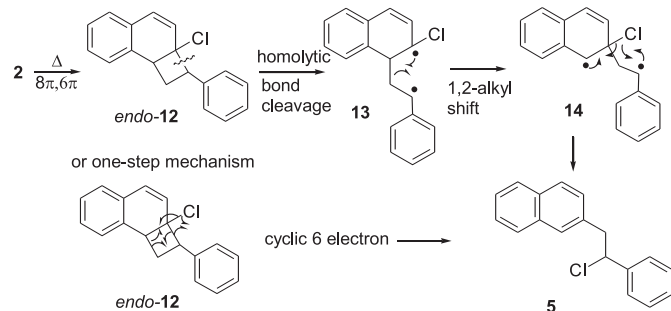


Fig. 4. ORTEP-3¹⁴ drawing of thermal product **11**. Displacement ellipsoids are drawn for the probability of 30% and hydrogen atoms are shown as spheres of arbitrary radii.

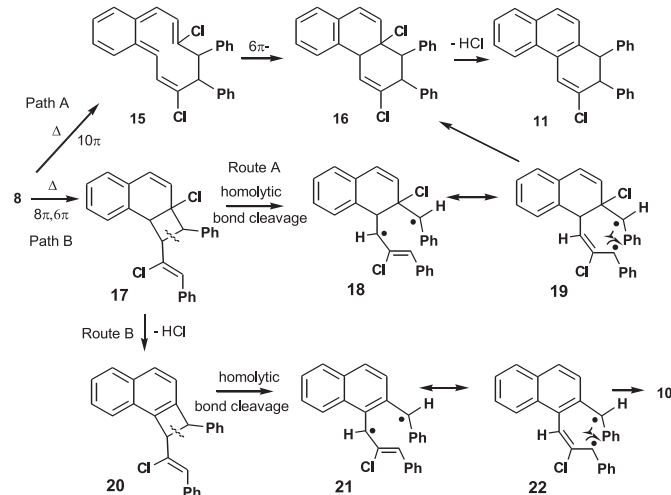
The molecular structure of **11** is shown in Fig. 4. The conformation of its central ring, C1 → C14 is between an envelope and screw-boat, as indicated by Cremer–Pople¹⁵ parameters: ring puckering amplitude is 0.419(3) Å, $\theta=114.5(4)^\circ$ and $\varphi=268.2(4)^\circ$. The 3D packing is achieved exclusively through C–H···π interactions (Table 1).

Differences in the chemical behavior of **1**, **2**, and **3** can be explained by the thermal instability of the initial product of 8π , 6π -electrocyclization *endo*-**12** (Scheme 3). Homolytic cleavage of cyclobutane ring gives biradical intermediate **13**, which undergoes 1,2-alkyl shift to form biradical **14**. Finally, 1,2-migration of chlorine followed by aromatization gives **5**. Alternatively, rearrangement of *endo*-**12** could take place in a single step via cyclic six electron shift. Homolytic cleavage of cyclobutane ring has its precedence in the elimination of styrene and formation of naphthalene described in one of our previous papers,¹¹ but was not detected in the case of **2**.



Scheme 3. Reaction mechanism for thermal reaction of benzoocataoctaene **2**.

The formation of product **11** could be envisaged by several reaction pathways shown in Scheme 4. The heating of **8** triggers the 10π -electrocyclization and formation of a cyclic intermediate **15** (Path A). Concomitant 6π -electrocyclization leads to **16**, which after elimination of hydrochloric acid aromatizes to 1,2-dihydrophenanthrene **11**. However, quantum-chemical calculations (B3LYP/6-31G*) for parent octatetraene indicated significantly lower activation barrier for 8π - than for 6π - or 10π -electrocyclization process (by 16.6 and 15.6 kJ mol^{−1}, respectively), suggesting that 8π -electrocyclization is the preferred pathway (Path B). In 8π , 6π -electrocyclization route product **17** is obtained, from which two pathways lead to final product **11**, depending on the timing of HCl elimination. If cyclobutene bond cleavage of **17** takes place first (Route A), biradical **18** is formed, which cyclizes to **17**. In the second route (B) HCl elimination and aromatization takes place first, followed by recombination to **11**. Chemical intuition favors the last reaction route, since aromatization of **17** gives a thermodynamically more stable product **20**, and also introduces additional ring strain in cyclobutene system, which promotes the ring opening process.



Scheme 4. Reaction mechanism for thermal reaction of benzodecapentaene **8**.

2.2. Quantum-chemical study

The origins of the experimentally observed *endo*-stereochemical outcomes of the thermal reactions of **1**, **2**, **6**, and **7** and additional support for structural assignments were sought computationally. Transition state calculations, using density functional theory (DFT) were employed using recently developed DFT functional M062X, which is specifically designed for obtaining better reaction energetics. A summary of the computational results is given in Fig. 5 and Table 2.

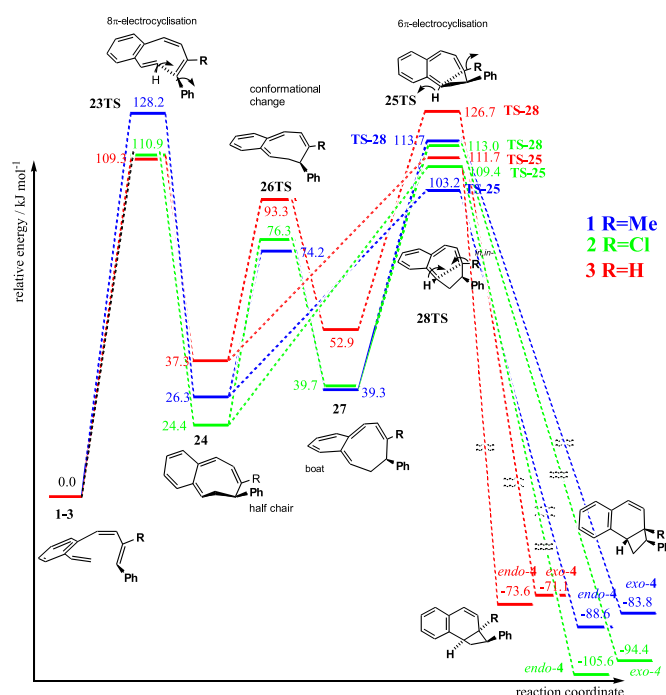


Fig. 5. Reaction energy profile for thermal electrocyclization of **1–3** calculated at the M06/6-311+G(d,p)//M06/6-31G(d)+ZPVE level of theory (kJ/mol).

Table 2

Relative energies (kJ/mol) calculated at the M06/6-311+G(d,p)//M06/6-31G(d)+ZPVE level of theory of **1–3** derivatives, with zero point energy corrections included

Molecule	1 (R=Me)	2 (R=Cl)	3 (R=H)
1–3	0.0	0.0	0.0
24-TS	109.2	110.9	128.2
25	26.3	24.4	37.3
26-TS	103.2	109.4	111.7
27-TS	80.5	76.3	93.3
28	39.3	39.7	52.9
29-TS	113.7	113.0	126.7
<i>endo</i> - 4	−88.6	−105.6	−73.6
<i>exo</i> - 4	−83.8	−94.4	−71.1

The proposed reaction mechanism for transformation of **1–3** to *endo/exo*-**4** involves an $8\pi,6\pi$ -electrocyclization cascade, (Fig. 5). In the first step (8π electrocyclization) conrotatory ring closure via transition state **23-TS** takes place, leading to an intermediate pentaaene **24**. The aromaticity of benzene moiety is restored in the second reaction step, (disrotatory 6π -electrocyclization), via **25-TS**, to form *endo*-**4**. To obtain the second possible isomeric product, *exo*-**4**, a conformational interconversion (ring flipping of the CH_2 group) of the intermediate **24** takes place via transition state **26-TS** to the boat conformer **27**. The disrotatory 6π -electrocyclization of **27** via transition state **28-TS**, leads to the product *exo*-**4**.

The obtained energy profile is similar to the one found in a previous study on structurally related benzoctatetraenes.¹¹ It shows a relatively small energy barrier is necessary for the conformational change **24**→**27** compared to electrocyclization processes. According to the Curtin–Hammett principle, the *endo/exo* product ratio is dictated by the relative heights of the energy barrier rather than the stabilities of the two intermediates. Subsequently the *endo*-**4** product is readily obtained via transition state **25-TS**, since the energy barrier for this reaction is lower than the barrier for the formation of *exo*-**4** products (via transition state **28-TS**) regardless of substituent (by 10.5, 4.6, and 15.0 kJ mol^{−1}, for **1**, **2**, and **3**, respectively). These results are in good accord with the experimentally observed exclusive formation of the *endo*-**4** product. Benzodecapentaene system **6** with additional olefinic bond behaves in similar manner as **3**, and *endo*-**9** is product preferred.

3. Conclusions

The thermal reactions of benzoctatetraenes and benzodecapentaenes substituted with R=H, Cl, and Me give different products depending on their substitution. In the case of H and Me substitution, the [4.2.0]bicyclooctadiene products of $8\pi,6\pi$ -electrocyclization are obtained. Chlorine substituted benzoctatetraene and benzodecapentaene gave unprecedented products, which are most likely formed by the thermal rearrangement of chlorine substituted products initially formed by $8\pi,6\pi$ -electrocyclization.

4. Experimental section

4.1. General

The ^1H spectra were recorded on a spectrometer at 600 MHz. The ^{13}C NMR spectra were registered at 150 MHz, respectively. All NMR spectra were measured in CDCl_3 using tetramethylsilane as reference. The assignment of the signals is based on 2D-CH correlation and 2D-HH-COSY experiments. UV spectra were measured on a UV/VIS Cary 50 spectrophotometer. IR spectra were recorded on a FTIR-ATR (film). Irradiation experiments were performed in a quartz vessel in toluene solution in a photochemical reactor equipped with 3000 Å lamps. All irradiation experiments were carried out in de-aerated solutions by passing a stream of argon prior to irradiation. Melting points were obtained using microscope equipped apparatus and are uncorrected. HRMS analysis were carried out on a mass spectrometer (MALDI TOF/TOF analyzer), equipped with Nd:YAG laser operating at 355 nm with firing rate 200 Hz in the positive (H^+) or negative (H^-) ion reflector mode. Silica gel (0.063–0.2 mm) was used for chromatographic purifications. Thin-layer chromatography (TLC) was performed silica gel 60 F₂₅₄ plates. Solvents were purified by distillation.

Cinnamaldehyde, α -methyl-cinnamaldehyde and α -chloro-cinnamaldehyde were obtained from a commercial source, β,β -*o*-xylyl(dtriphenylphosphonium)dibromide was prepared from *o*-xylyldibromide and triphenylphosphine in dimethylformamide.

4.2. (1E,3E)-2-Methyl-1-phenyl-4-(*o*-styrenyl)-1,3-butadiene (1); (1Z,3E)-2-chloro-1-phenyl-4-(*o*-styrenyl)-1,3-butadiene (2)

Starting compounds **1** and **2** were prepared by Wittig reaction¹³ from *o*-xylylenebis(triphenylphosphonium bromide) and the corresponding aldehydes, α -chloro-cinnamaldehyde and α -methyl-cinnamaldehyde. To a stirred solution of the triphenylphosphonium salt (0.001 mol) and the corresponding aldehyde (0.011 mol) in absolute ethanol (200 mL), a solution of sodium ethoxide (0.253 g, 0.011 mol in 15 mL of absolute ethanol) was added dropwise. Stirring was continued under a stream of nitrogen for

one hour at rt. Under the stream of dry nitrogen gaseous formaldehyde (obtained by decomposition of paraformaldehyde taken in excess, 1.5 g) was introduced and the next quantity of sodium ethoxide (0.253 g, 0.011 mol) in absolute ethanol (15 mL) was added dropwise. The reaction was completed within 3–4 h (usually was left to stand overnight). After removal of the solvent, the residue was worked up with water and toluene. The toluene extracts were dried (anhydrous MgSO₄) and concentrated. The crude reaction mixture was purified and the isomers of products **1** and **2** were separated by repeated column chromatography on silica gel using petroleum ether as the eluent. The first fractions yielded *cis*- and the last fractions *trans*-isomers.

4.3. General procedure for thermal reactions of **1** and **2**

A solution of *cis*-**1** (0.05 g, 0.00019 mol) or *cis*-**2** (0.05 g, 0.00020 mol) was dissolved in toluene (25 mL) and refluxed for 16 h. The solvent was removed in vacuo and the residue was chromatographed on a silica gel column using petroleum ether as the eluent. In the first fractions the thermal products *endo*-**4** (45 mg, 90%) or **5** (45 mg, 90%) were isolated.

4.3.1. 5-Methyl-4-phenyltricyclo[6.4.0^{2,5}]dodeca-1(8),6,9,11-tetraene (*endo*-4**).** *R*_f (petroleum ether) 0.36; colorless oil; UV (EtOH) λ_{max} (log ϵ) 322 (3.22, sh), 277 (3.90, sh), 270 (3.92); δ_{H} (600 MHz, CDCl₃) δ 7.30 (t, *J*=7.7 Hz, 2H, H-ar), 7.21 (t, *J*=7.7 Hz, 1H, H-ar), 7.21 (d, *J*=7.7 Hz, 2H, H-ar), 7.12 (d, *J*=8.6 Hz, 2H, H-ar), 7.00–7.02 (m, 2H), 6.32 (d, *J*=9.9 Hz, 1H, H-A), 5.11 (d, *J*=9.9 Hz, 1H, H-B), 3.61 (dd, *J*=7.7, 11.2 Hz, 1H, H-C), 3.25 (t, *J*=9.1 Hz, 1H, H-D), 2.50–2.57 (m, 1H, H-E), 2.28–2.40 (m, 1H, H-F), 1.32 (s, 3H, –CH₃); δ_{C} (150 MHz, CDCl₃) 138.7 (s), 135.1 (s), 131.6 (2d), 127.6 (2d), 127.1 (2d), 126.6 (d), 126.5 (d), 126.3 (d), 125.8 (d), 125.8 (d), 53.2 (d), 41.0 (d), 30.5 (t), 27.5 (q); ν_{max} (evaporated film from CHCl₃) 2943, 1452, 698 cm⁻¹; HRMS MH⁺, found 245.1346. C₁₉H₁₈ requires 245.1336.

4.3.2. 1-Chloro-2-(2-naphthyl)-1-phenylethane (5**).** *R*_f (petroleum ether) 0.15; colorless crystals; mp 57–59 °C; UV (EtOH) λ_{max} (log ϵ) 332 (3.36), 318 (3.48), 306 (3.41), 288 (3.69, sh), 278 (3.85), 270 (3.84), 261 (3.73, sh); δ_{H} (600 MHz, CDCl₃) 7.81 (dd, *J*=7.7, 1.7 Hz, 1H, H-ar), 7.76 (t, *J*=8.6 Hz, 2H, H-ar), 7.60 (s, 1H), 7.44–7.49 (m, 2H), 7.40 (d, *J*=7.7 Hz, 2H), 7.30–7.37 (m, 3H), 7.25 (dd, *J*=8.6, 1.2 Hz, 1H, H-ar), 5.15 (t, *J*=7.4 Hz, 1H, H-A), 3.55 (dd, *J*=7.4, 14.0 Hz, 1H, H-B/H-C), 3.50 (dd, *J*=7.4, 14.0 Hz, 1H, H-B/H-C); δ_{C} (150 MHz, CDCl₃) 140.6 (s), 134.5 (s), 132.9 (s), 131.9 (s), 128.1 (2d), 127.9 (d), 127.7 (d), 127.4 (d), 127.1 (d), 127.1 (d), 127.0 (d), 126.7 (d), 125.5 (d), 125.1 (2d), 63.5 (d), 46.2 (t); ν_{max} (evaporated film from CHCl₃) 2924, 1725, 1453, 697 cm⁻¹; HRMS M⁺, found 266.0853. C₁₈H₁₅Cl requires 266.0857.

4.4. (1E,3E)-1-{*o*-[(1E,3E)-4-Phenyl-1,3-butadienyl]phenyl}-4-phenyl-1,3-butadiene (6**); (1E,3E)-4-{*o*-[(1E,3E)-3-Methyl-4-phenyl-1,3-butadienyl]phenyl}-2-methyl-1-phenyl-1,3-butadiene (**7**); (1Z,3E)-4-{*o*-[(1E,3Z)-3-chloro-4-phenyl-1,3-butadienyl]phenyl}-2-chloro-1-phenyl-1,3-butadiene (**8**)¹³**

To a stirred solution of the triphenylphosphonium salt (0.005 mol) and the corresponding aldehyde (0.011 mol) in absolute ethanol (100 mL) a solution of sodium ethoxide (0.253 g, 0.011 mol in 15 mL of absolute ethanol) was added dropwise. The reaction was completed within 3–4 h (usually was left to stand overnight). After removal of the solvent, the residue was worked up with water and toluene. The toluene extracts were dried (anhydrous MgSO₄) and concentrated. The crude reaction mixture was purified and the isomers of products **6**, **7**, and **8** were separated by repeated column chromatography on silica gel using petroleum ether as the eluent. The first fractions yielded *cis,cis*-, *cis,trans*- and the last fractions *trans,trans*-isomers.

4.5. General procedure for thermal reactions of **6**–**8**

A mixture of *cis,cis*-**6**–**8** and *cis,trans*-**6**–**8** (0.05 g; **6**: 0.00015 mol, **7**: 0.00012 mol, **8**: 0.00015 mol) was dissolved in toluene (25 mL) and refluxed for 8 h. Solvent was removed in vacuo and the residue was chromatographed on a silica gel column using petroleum ether as the eluent. In the first fractions the thermal products **9** (0.040 g, 20%), **10** (0.020 g, 40%) or **11** (0.030 g, 60%) were isolated.

4.5.1. 3-[*(E*)-2-Phenylethenyl]-4-phenyltricyclo[6.4.0^{2,5}]dodeca-1(8),6,9,11-tetraene (*endo*-9**).** *R*_f (30% CH₂Cl₂/petroleum ether) 0.56; colorless crystals; mp 142–145 °C; UV (EtOH) λ_{max} (log ϵ) 263 (4.01); δ_{H} (600 MHz, CDCl₃) 7.55 (d, *J*=7.6 Hz, 1H), 7.32 (dt, *J*=7.6, 0.9 Hz, 1H), 7.24–7.28 (m, 5H), 7.13 (d, *J*=7.6 Hz, 1H), 7.10 (t, *J*=7.6 Hz, 1H), 7.05 (d, *J*=7.6 Hz, 1H), 6.99 (t, *J*=7.6 Hz, 2H), 6.65–6.70 (m, 3H), 6.44 (dd, *J*=9.6, 2.6 Hz, 1H, H-A), 6.04–6.08 (m, 1H), 5.72 (dd, *J*=9.6, 1.7 Hz, 1H, H-B), 3.74 (t, *J*=5.1 Hz, 1H, H-C/H-D), 3.54 (d, *J*=14.3 Hz, 1H, H-C/H-D), 3.44 (dd, *J*=12.5, 5.9 Hz, 1H, H-E/H-F), 2.81 (ddd, *J*=14.3, 12.5, 4.1 Hz, 1H, H-E/H-F); δ_{C} (150 MHz, CDCl₃) 140.1 (s), 139.0 (s), 137.4 (s), 134.4 (s), 132.7 (d), 130.0 (2d), 130.0 (d), 127.6 (d), 126.7 (3d), 125.9 (d), 125.8 (d), 125.7 (d), 125.6 (d), 125.5 (d), 122.3 (d), 49.1 (d), 48.5 (d), 41.7 (d), 33.4 (d); ν_{max} (evaporated film from CHCl₃) 2923, 1677, 1493, 693 cm⁻¹; HRMS MH⁺, found 335.1759. C₂₆H₂₂ requires 335.1749.

4.5.2. 3-[*(E*)-1-Methyl-2-phenylethenyl]-5-methyl-4-phenyl tricyclo[6.4.0^{2,5}]dodeca-1(8),6,9,11-tetraene (*endo*-10**).** *R*_f (30% CH₂Cl₂/petroleum ether) 0.56; colorless oil; UV (EtOH) λ_{max} (log ϵ) 323 (3.54), 256 (4.24); δ_{H} (600 MHz, CDCl₃) 7.31–7.35 (m, 3H), 7.26–7.30 (m, 4H), 7.22–7.25 (m, 1H), 7.20 (d, *J*=7.3 Hz, 2H), 7.13–7.17 (m, 2H), 7.07 (dd, *J*=7.1, 1.6 Hz, 1H), 7.05 (dd, *J*=7.1, 1.6 Hz, 1H), 6.36 (d, *J*=10.0 Hz, H-A), 6.34 (s, 1H), 5.20 (d, *J*=10.0 Hz, 1H, H-B), 3.60 (d, *J*=9.0 Hz, 1H, H-C/H-E), 3.54 (t, *J*=9.0 Hz, 1H, H-F), 3.23 (d, *J*=9.0 Hz, 1H, H-C/H-E), 1.81 (d, *J*=0.6 Hz, 3H, –CH₃'), 1.35 (s, –CH₃); δ_{C} (150 MHz, CDCl₃) 138.5 (s), 138.0 (s), 137.7 (s), 134.1 (s), 132.1 (d), 131.8 (s), 131.7 (s), 128.5 (d), 127.8 (d, d), 127.7 (d), 127.5 (2d), 127.3 (2d), 127.0 (d), 126.6 (d), 126.5 (d), 126.0 (d), 125.8 (d), 125.5 (d), 123.9 (d), 57.4 (d), 50.8 (d), 47.1 (d), 27.3 (q), 16.1 (q); ν_{max} (evaporated film from CHCl₃) 3023, 1600, 1493, 700 cm⁻¹; HRMS M⁺, found 362.2035. C₂₈H₂₆ requires 362.2029.

4.5.3. 3-Chloro-1,2-diphenyl-1,2-dihydrophenanthrene (11**).** *R*_f (30% CH₂Cl₂/petroleum ether) 0.56; colorless crystals; mp 100–102 °C; UV (EtOH) λ_{max} (log ϵ) 342 (3.98), 326 (4.07), 312 (3.94), 245 (4.74); δ_{H} (600 MHz, CDCl₃) 8.24 (d, *J*=7.9 Hz, 1H), 7.82 (d, *J*=7.9 Hz, 1H), 7.74 (s, 1H), 7.57–7.62 (m, 2H), 7.50 (t, *J*=7.9 Hz, 1H), 7.21 (t, *J*=7.3 Hz, 1H), 7.11–7.16 (m, 3H), 6.99–7.04 (m, 3H), 6.71–6.78 (m, 2H), 5.02 (d, *J*=8.0 Hz, H₁, 1H), 3.88 (d, *J*=8.0 Hz, H₂, 1H); δ_{C} (150 MHz, CDCl₃) 137.9 (s), 136.0 (s), 135.3 (s), 135.1 (s), 133.1 (s), 132.3 (s), 129.7 (s), 128.5 (s), 128.3 (s), 130.2 (2d), 128.9 (d), 128.1 (d), 127.4 (2d), 127.3 (d), 127.2 (d), 127.0 (d), 126.5 (d), 126.0 (d), 125.5 (d), 125.1 (d), 121.9 (d), 121.4 (d), 54.4 (d), 53.0 (d); ν_{max} (evaporated film from CHCl₃) 2923, 1738, 1452, 698 cm⁻¹; HRMS M⁺, found 365.1095. C₂₆H₁₉Cl requires 365.1091.

Single crystal measurements were performed on an Oxford Diffraction Xcalibur Nova R (microfocus Cu tube) at room temperature [293(2) K]. Program package CrysAlis PRO¹⁶ was used for data reduction. The structure was solved using SHELXS97 and refined with SHELXL97.¹⁷ The model was refined using the full-matrix least squares refinement; all non-hydrogen atoms were refined anisotropically. Hydrogen atoms were modeled as riding entities using the AFIX command. Due to the disorder (see Section 2.1) and the small size of the crystal (Fig. S1, Table 1) data for **5** were of somewhat inferior quality. Molecular geometry calculations were performed by PLATON,¹⁸ and molecular graphics were prepared using

ORTEP-3,¹⁴ and CCDC-Mercury.¹⁹ Crystallographic and refinement data for the structures reported in this paper are shown in **Supplementary data, Table 1**.

4.5.3.1. Computational details. All computational studies reported in this work were performed using the Gaussian09 program,²⁰ implemented on dual core Opteron 240 personal computer under Linux operating system and computer cluster Isabella at the Computing center of the University of Zagreb within the density functional theory (DFT) framework. Both B3LYP and M06-2X hybrid functionals were used along with the 6-31G(d) and 6-311+G(d,p) basis sets. All the stationary points were characterized by harmonic analysis and activation energies were computed including zero-point vibrational energy corrections.

Acknowledgements

This research was funded by grants from the Croatian Ministry of Science, Education and Sports (125-0982933-2926, 098-0982929-2917, 098-1191344-2943 and 098-0982933-3218). The computing center of the Zagreb University is thanked for allocating the time at the computer cluster Isabella.

Supplementary data

Supplementary crystallographic data for this paper can be obtained free of charge via www.ccdc.cam.ac.uk/conts/retrieving.html (or from the Cambridge Crystallographic Data Centre, 12, Union Road, Cambridge CB2 1EZ, UK; fax: +44 1223 336033; or deposit@ccdc.cam.ac.uk). CCDC-963633 and 963634 contain the supplementary crystallographic data for this paper. Supplementary data related to this article can be found at <http://dx.doi.org/10.1016/j.tet.2013.12.027>.

References and notes

1. *The Chemistry of Dienes and Polyenes*; Rappoport, Z., Ed.; Wiley: Chichester, UK, 2000; Vol. 2.
2. Burnley, J.; Ralph, M.; Sharma, P.; Moses, J. E. In *Biomimetic Organic Synthesis*; Poupon, E., Nay, B., Eds.; Wiley: Weinheim, Germany, 2011; Vol. 1, pp 591–636.
3. Oxaelectrocyclization: Fotiadou, A. D.; Zografos, A. L. *Org. Lett.* **2012**, *16*, 5664–5667.
4. Azaelectrocyclization: Cheng, X.; Waters, S. P. *Org. Lett.* **2013**, *15*, 4226–4229.
5. Kim, K.; Lauher, J. W.; Parker, K. A. *Org. Lett.* **2012**, *14*, 138–141.
6. Sofiyev, V.; Navarro, G.; Trauner, D. *Org. Lett.* **2008**, *10*, 149–152.
7. Sharma, P.; Ritson, D. J.; Burnley, J.; Moses, J. E. *Chem. Commun.* **2011**, 10605–10607.
8. Shang, M.; Butler, D. N.; Warrener, R. N.; Margetić, D. *Tetrahedron Lett.* **2013**, *54*, 5335–5337; Margetić, D.; Warrener, R. N.; Butler, D. N.; Jin, C.-M. *Tetrahedron* **2012**, *68*, 3306–3318; Margetić, D.; Butler, D. N.; Warrener, R. N.; Murata, Y. *Tetrahedron* **2011**, *67*, 1580–1588; Margetić, D.; Eckert-Maksic, M.; Trošelj, P.; Marinić, Ž. *J. Flou. Chem.* **2010**, *131*, 408–416; Margetić, D.; Warrener, R. N.; Butler, D. N. *Aust. J. Chem.* **2000**, *53*, 959–963.
9. Kikaš, I.; Škorić, I.; Marinić, Ž.; Sindler-Kulyk, M. *Tetrahedron* **2010**, *66*, 9405–9414; Vidaković, D.; Škorić, I.; Horvat, M.; Marinić, Ž.; Sindler-Kulyk, M. *Tetrahedron* **2008**, *64*, 3928–3934; Basarić, N.; Marinić, Ž.; Sindler-Kulyk, M. *J. Org. Chem.* **2006**, *71*, 9382–9392; Škorić, I.; Flegar, I.; Marinić, Ž.; Sindler-Kulyk, M. *Tetrahedron* **2006**, *62*, 7396–7407; Škorić, I.; Basarić, N.; Marinić, Ž.; Višnjevac, A.; Kojić-Prodić, B.; Sindler-Kulyk, M. *Chem.—Eur. J.* **2005**, *11*, 543–551; Butković, K.; Basarić, N.; Lovreković, K.; Marinić, Ž.; Višnjevac, A.; Kojić-Prodić, B.; Sindler-Kulyk, M. *Tetrahedron Lett.* **2004**, *45*, 9057–9060.
10. Škorić, I.; Šmehil, M.; Marinić, Ž.; Molčanov, K.; Kojić-Prodić, B.; Sindler-Kulyk, M. *J. Photochem. Photobiol. A: Chem.* **2009**, *207*, 190–196.
11. Škorić, I.; Pavlović, F.; Marinić, Ž.; Sindler, M.; Eckert-Maksic, M.; Vazdar, M.; Margetić, D. *Org. Biomol. Chem.* **2011**, *9*, 6771–6778.
12. Sindler-Kulyk, M.; Stiplošek, Z.; Vojnović, D.; Metelko, B.; Marinić, Ž. *Heterocycles* **1991**, *32*, 2357–2363.
13. Škorić, I.; Kikaš, I.; Kovács, M.; Fodor, L.; Marinić, Ž.; Molčanov, K.; Kojić-Prodić, B.; Horváth, O. J. *Org. Chem.* **2011**, *21*, 8641–8657; Kikaš, I.; Horváth, O.; Škorić, I. *J. Mol. Struct.* **2013**, *1034*, 62–68.
14. Farrugia, L. J. *J. Appl. Crystallogr.* **1997**, *30*, 565–566.
15. Cremer, D.; Pople, J. A. *J. Am. Chem. Soc.* **1975**, *97*, 1354–1358.
16. CrysAlis PRO; Oxford Diffraction Ltd: U.K., 2007.
17. Sheldrick, G. M. *Acta Crystallogr.* **2008**, *A64*, 112–122.
18. PLATON: Spek, A. L. *J. Appl. Crystallogr.* **2003**, *36*, 7–13.
19. Macrae, C. F.; Edgington, P. R.; McCabe, P.; Pidcock, E.; Shields, G. P.; Taylor, R.; Towler, M.; van de Streek, J. *J. Appl. Crystallogr.* **2006**, *39*, 453–457.
20. Frisch, M. J.; Trucks, G. W.; Schlegel, H. B.; Scuseria, G. E.; Robb, M. A.; Cheeseman, J. R.; Scalmani, G.; Barone, V.; Mennucci, B.; Petersson, G. A.; Nakatsuji, H.; Caricato, M.; Li, X.; Hratchian, H. P.; Izmaylov, A. F.; Bloino, J.; Zheng, G.; Sonnenberg, J. L.; Hada, M.; Ehara, M.; Toyota, K.; Fukuda, R.; Hasegawa, J.; Ishida, M.; Nakajima, T.; Honda, Y.; Kitao, O.; Nakai, H.; Vreven, T.; Montgomery, J. A., Jr.; Peralta, J. E.; Ogliaro, F.; Bearpark, M.; Heyd, J. J.; Brothers, E.; Kudin, K. N.; Staroverov, V. N.; Kobayashi, R.; Normand, J.; Raghavachari, K.; Rendell, A.; Burant, J. C.; Iyengar, S. S.; Tomasi, J.; Cossi, M.; Rega, N.; Millam, N. J.; Klene, M.; Knox, J. E.; Cross, J. B.; Bakken, V.; Adamo, C.; Jaramillo, J.; Gomperts, R.; Stratmann, R. E.; Yazyev, O.; Austin, A. J.; Cammi, R.; Pomelli, C.; Ochterski, J. W.; Martin, R. L.; Morokuma, K.; Zakrzewski, V. G.; Voth, G. A.; Salvador, P.; Dannenberg, J. J.; Dapprich, S.; Daniels, A. D.; Farkas, Ö.; Foresman, J. B.; Ortiz, J. V.; Cioslowski, J.; Fox, D. J. *Gaussian 09, Revision A.1*; Gaussian: Wallingford CT, 2009.